Progress In Electromagnetics Research M, Vol. 118, 59–69, 2023

Time Domain Modeling Method for the Coupling Analysis of Branched Lines Excited by Ambient Wave

Zhihong Ye[1, 2, *], Xin Xia[1], Changchang Lu[1], and Yu Zhang[1]

Abstract—An efficient time domain hybrid method, consisting of the finite-difference time-domain (FDTD) method, Norton's theorem, transmission line (TL) equations, and some interpolation techniques, is presented to realize the fast coupling simulation of branched lines (BLs) radiated by ambient wave. Firstly, the branched lines are decomposed into multiple independent multi-conductor transmission lines (MTLs) according to the branched nodes. Then the TL equations with interpolation techniques are employed to build the coupling model of each MTL. The transient responses on these MTLs are solved by the FDTD method, which are employed to extract the Norton circuits of these MTLs acting on the branched nodes according to the Norton's theorem. Finally, the correlation matrix of the voltages and currents at the ports of the branched nodes is derived and solved. Meanwhile, these voltages are fed back to the corresponding MTLs as boundaries to realize the interference signal transmission among the BLs. Numerical examples about the coupling of branched lines contributed by five wires in free space and complex environment are simulated and compared with that of traditional FDTD to verify the correctness and efficiency of this proposed method.

1. INTRODUCTION

Various types of transmission lines are the crucial components of electronic and electric systems to realize the data communication between different devices. To compress the space occupied by the transmission lines, they must be bundled and then branched to connect to different devices. This shape of the transmission lines is called as branched lines. Therefore, studying the coupling problem of space electromagnetic fields acting on the branched lines is significant for the electromagnetic safety evaluations of the electronic and electric systems.

Some field-line coupling methods have been proposed to deal with the coupling problem of the TLs efficiently, such as Baum-Liu-Tesche (BLT) equation [1–4], FDTD-SPICE method [5–9], and FDTD-TL method [10–13]. The common advantage of these methods is that they can avoid direct mesh division of the fine structures of TLs. However, the BLT equation can only obtain a single frequency response on the TLs via once computation. Its computation efficiency will be deeply decreased when the ambient wave is a broadband signal, and the network scale of the TLs is large. Even though the time domain BLT equation has been studied [16], a number of convolution operations are required, which should raise the computational complexity apparently. FDTD-SPICE and FDTD-TL are both time-domain algorithms and widely applied to the coupling analysis of the transmission line network excited by broadband pulse signals. However, FDTD-SPICE requires tedious theoretical derivation when establishing the SPICE equivalent circuit model of the TL network; meanwhile, the space electromagnetic fields and the transient responses on the TL network need to be calculated respectively. It will cause a sharp decline in the computation efficiency of this method with the increase of calculation time. The feature

Received 1 April 2023, Accepted 14 June 2023, Scheduled 25 July 2023
* Corresponding author: Zhihong Ye (yezh@cqupt.edu.cn).
[1] School of Communication and Information Engineering, Chongqing University of Posts and Telecommunications, Chongqing 400065, China. [2] Chongqing Institute of Digital Arena, Chongqing 400065, China.

advantage of the FDTD-TL method is that it can synchronously compute the space electromagnetic fields and the transient responses of the TL network. Hence, we have employed the FDTD-TL method to deal with the coupling problems of the oblique transmission line and its network efficiently [14, 15]. In these studies, the coupling model of the TL with arbitrary direction is constructed, and the interference signal transmission between these single TLs of the TL network is realized by the application of Norton's theorem. However, the coupling analysis of the TL network contributed by multiconductor transmission lines and containing branched structures cannot be directly solved via our previous researches.

Therefore, based on the FDTD-TL method and combined with the Norton's theorem and interpolation techniques, a time domain hybrid method is presented for the coupling analysis of the branched lines efficiently. The detailed implementation process of this proposed method will be introduced as follows.

2. THEORY OF THE HYBRID METHOD

The typical coupling model of branched lines excited by ambient wave is shown in Fig. 1. It is assumed that the BLs are located on a perfect conductor (PEC) ground, and the BLs are composed of several MTL segments which are connected with each other via the branched nodes. In this work, the skin effect of the BLs is not considered. It means that the loss of the BLs is ignored.

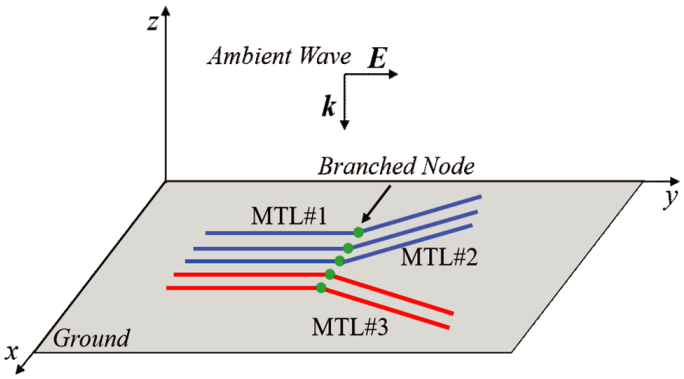

Figure 1. Coupling model of ambient wave acting on the branched lines.

The proposed time domain hybrid method applied to the coupling analysis of the BLs includes three steps.

Firstly, the whole structure of the BLs is decomposed into several independent MTLs and branched nodes.

Secondly, the coupling models of space electromagnetic fields to these MTLs are constructed by the TL equations combined with some interpolation techniques, and then the TL equations are solved by the FDTD to obtain the transient responses on these MTLs.

Finally, owing to the Norton's theorem, the effects of these MTLs on the branched nodes can be equivalent to Norton circuits, and the equivalent multi-port network considering the coupling of these branched nodes is constructed. Then the admittance matrix representing the V-I relationship of this multi-port network is constructed and solved to obtain the port voltages of the branched nodes, which are fed back to the MTLs as boundaries to realize the interference signal transmission among the BLs.

Next, the implementation process of this proposed method will be introduced in detail from two aspects of the coupling analysis of each MTLs and the equivalent circuit modeling of branched nodes. In order to clearly explain our method, the BL model contributed by five transmission lines and split to two sub MTL segments is employed, where the three MTL segments are named as MTL#1, MTL#2, and MTL#3, as shown in Fig. 1. Meanwhile, the coupling effect between MTL#2 and MTL#3 can be neglected under the condition that the angle between the directions of the two MTLs is large enough, because the mutual effects between the MTLs are weak with the increase of the distance of the MTLs.

2.1. Coupling Analysis of Each MTLs

The time domain TL equations representing the coupling of space electromagnetic fields to each MTLs are expressed as

$$\frac{\partial}{\partial l}\mathbf{V}(l,t)+\mathbf{L}\frac{\partial}{\partial t}\mathbf{I}(l,t) = \mathbf{V}_{\mathrm{F}}(l,t) \tag{1}$$

$$\frac{\partial}{\partial l}\mathbf{I}(l,t)+\mathbf{C}\frac{\partial}{\partial t}\mathbf{V}(l,t) = \mathbf{I}_{\mathrm{F}}(l,t) \tag{2}$$

where l represents the direction of each MTLs. $\mathbf{V}(l,t)$ and $\mathbf{I}(l,t)$ represent the voltage and current vectors on the MTLs. $\mathbf{L}$ and $\mathbf{C}$ are the per unit length inductance and capacitance matrices of the MTLs, respectively, which can be calculated via the empirical formulas found from [17]. $\mathbf{V}_{\mathrm{F}}(l,t)$ and $\mathbf{I}_{\mathrm{F}}(l,t)$ are the distributed voltage and current source terms of the TL equations, which can be expressed as

$$\mathbf{V}_{\mathrm{F}}(l,t) = -\frac{\partial}{\partial l}\mathbf{E}_{\mathrm{T}}(l,t)+\mathbf{E}_{\mathrm{L}}(l,t) \tag{3}$$

$$\mathbf{I}_{\mathrm{F}}(l,t) = -\mathbf{C}\frac{\partial}{\partial t}\mathbf{E}_{\mathrm{T}}(l,t) \tag{4}$$

where $\mathbf{E}_{\mathrm{T}}(l,t)$ and $\mathbf{E}_{\mathrm{L}}(l,t)$ are obtained from the space electromagnetic fields, which are expressed as

$$[\mathbf{E}_{\mathrm{T}}(l,t)]_i = \int_0^{h_i} e_z^{ex}(x,y,z,t)\,dz \tag{5}$$

$$[\mathbf{E}_{\mathrm{L}}(l,t)]_i = e_l^{ex}(x,y,h_i,t)-e_l^{ex}(x,y,0,t) \tag{6}$$

where h_i represents the distance of the i-th TL of the MTLs to the ground. $[\mathbf{E}_{\mathrm{T}}(l,t)]_i$ is the integral of the incident electric field component e_z^{ex} vertical to the i-th TL, and $[\mathbf{E}_{\mathrm{L}}(l,t)]_i$ is the difference of the tangential electric field components e_l^{ex} along the i-th TL and the surface of the ground. Because the equivalent distributed source terms of TL equations are independent of the scattering fields of the MTLs, the MTLs can be removed when the incident electromagnetic fields are calculated.

Because the directions of these MTL segments are different, and the heights of these MTLs may be arbitrary values, the MTL structures cannot be entirely located on the edges of FDTD grids. Under the circumstance, the incident electric fields along and vertical to the MTLs should be obtained by the interpolation of the electric fields on the FDTD grids.

Firstly, the electric fields on the FDTD grids are utilized to obtain the tangential electric fields along the MTLs to get the values of $\mathbf{E}_{\mathrm{L}}(l,t)$ via some interpolation schemes. When the MTLs are meshed by the FDTD grid into multiple MTL segments, the starting and ending points of each line of every MTL segment are located on the face of FDTD grid, and the center point of the line is just located on the central plane of FDTD grid, as shown in Fig. 2. Then, the electric field along the line at the center point can be obtained via the dot product operation of the electric field vector $\mathbf{E}$ at

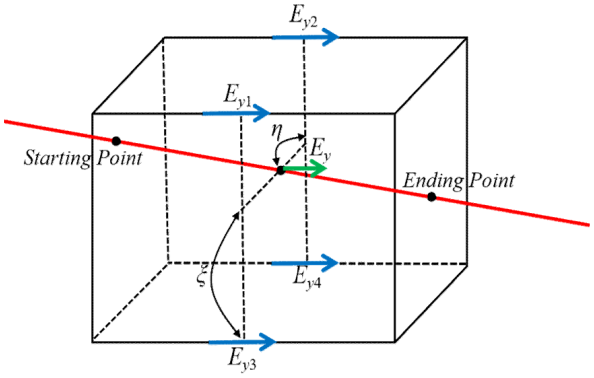

Figure 2. Interpolation scheme for the tangential electric fields of the MTLs.

the center point of the line and the unit direction vector $\mathbf{e}_l$ of the line, which is expressed as $\mathbf{E} \cdot \mathbf{e}_l$. Here, $\mathbf{e}_l$ is established via the coordinates of the starting and ending points. $\mathbf{E}$ is contributed by three electric field components E_x, E_y, and E_z at the center point of the line, which should be obtained by the interpolation of the corresponding electric field components on its and adjacent FDTD grids. Here, taking E_y as an example, the interpolation formula can be expressed as

$$E_y = (1-\eta)\left[\xi E_{y1} + (1-\xi) E_{y3}\right] + \eta\left[\xi E_{y2} + (1-\xi) E_{y4}\right] \tag{7}$$

where E_{y1}, E_{y2}, E_{y3}, and E_{y4} are the electric field components on the edges of the FDTD grid. η and ξ are the scale factors of the center point in the FDTD grid, respectively. If the coordinates of this center point and the starting position of the whole computation region are assumed as (x_s, y_s, z_s) and (x_m, y_m, z_m), the scale factors η and ξ are computed by $\eta = (x_s - x_m)/\Delta x - \text{int}\left[(x_s - x_m)/\Delta x\right]$ and $\xi = (z_s - z_m)/\Delta z - \text{int}\left[(z_s - z_m)/\Delta z\right]$, respectively, where Δx and Δz are the space steps used by the FDTD, and int $[\cdot]$ stands for the rounding operation.

E_x and E_z should be interpolated from eight electric fields on the edges of its and adjacent FDTD grids, and the detailed interpolation formulas can be found from [14].

Then, the vertical electric fields of the line are interpolated from the electric fields on the FDTD grids and integrated to obtain the values of $\mathbf{E}_{\mathrm{T}}(l,t)$. As shown in Fig. 3, two electric fields E_z on the edges of the FDTD grid are used to obtain the electric field component E_z^{inc} via the interpolation scheme, which is expressed as

$$E_z^{inc} = \alpha E_{z3} + (1-\alpha) E_{z4} \tag{8}$$

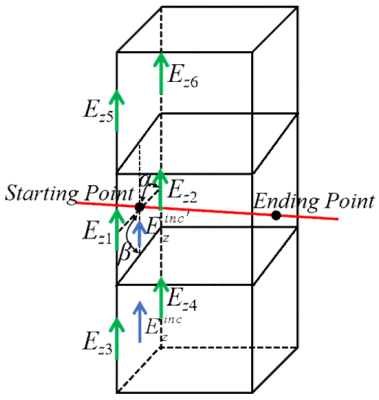

Figure 3. Interpolation scheme for the vertical electric fields of the MTLs.

The electric field $E_z^{inc'}$ adjacent to the line needs to be interpolated from four electric fields E_z on the edges of its and adjacent FDTD grids, which is expressed as

$$E_z^{inc'} = \begin{cases} \left[(0.5+\beta)\left[\alpha E_{z1} + (1-\alpha) E_{z2}\right] + (0.5-\beta)\left[\alpha E_{z3} + (1-\alpha) E_{z4}\right]\right] & \beta < 0.5 \\ \left[(1.5-\beta)\left[\alpha E_{z1} + (1-\alpha) E_{z2}\right] + (\beta-0.5)\left[\alpha E_{z5} + (1-\alpha) E_{z6}\right]\right] & \beta \geq 0.5 \end{cases} \tag{9}$$

where α and β are the scale factors for the positions of the starting or ending points in the FDTD grid. If the coordinate of this starting point is set as (x_n, y_n, z_n), the scale factors α and β are computed by $\alpha = (x_n - x_m)/\Delta x - \text{int}\left[(x_n - x_m)/\Delta x\right]$ and $\beta = (z_n - z_m)/\Delta z - \text{int}\left[(z_n - z_m)/\Delta z\right]$, respectively.

When the calculation of the distributed source terms is completed, the TL equations are established. Then, the FDTD's central difference scheme is utilized to discretize the TL equations to obtain the transient voltage and current responses on the MTLs and their terminal loads.

2.2. Equivalent Circuit Modeling of Branched Nodes

Because the port voltages of these MTLs connecting to the branched nodes cannot be discretized and solved by the FDTD's central difference scheme, forward and backward difference schemes are appropriate ways for the solutions of these voltages. Here, taking the terminal voltage V_{N} of one line

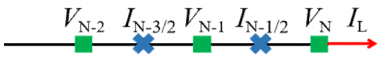

Figure 4. Port voltage V_N solved by the backward difference scheme.

of MTL#1 as an example, the current flowing into the branched node is assumed as I_L, as shown in Fig. 4, where N is the node number of the voltages on this line. Then the backward difference scheme is employed to discretize Equation (2) where the source term $\boldsymbol{I}_F$ at terminal position is zero, which is expressed as

$$\frac{1}{\Delta l_1/2}\left(\frac{I_L^{n+1}+I_L^n}{2}-I_{N-\frac{1}{2}}^{n+\frac{1}{2}}\right)+C_e\frac{V_N^{n+1}-V_N^n}{\Delta t}=0 \tag{10}$$

where n represents the current time step, C_e the self capacitance of this line, Δl_1 the grid size of MTL#1 under the division of the FDTD grid, and Δt the time step of the FDTD.

Thus, the calculation formula of current I_L can be arranged as

$$I_L^{n+1}=I_{LH}^{n+1/2}+G_{eq}V_N^{n+1} \tag{11}$$

where

$$G_{eq} = \Delta l_1\frac{C_e}{\Delta t} \tag{12}$$

$$I_{LH}^{n+1/2} = -2I_{N-1/2}^{n+1/2}-I_L^n-G_{eq}V_N^n \tag{13}$$

It can be seen from Equation (11) that the effect of this line to the branched node can be equivalent to a Norton circuit, as shown in Fig. 5, where the circuit consists of a current source I_{LH} and equivalent admittance G_{eq}.

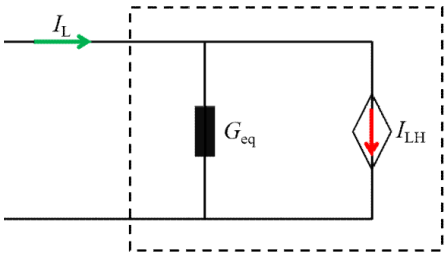

Figure 5. Norton equivalent circuit.

On the basis, the effects of these MTLs on the branched nodes can also be equivalent to Norton circuits, and then the whole equivalent circuit model of the branched nodes is constructed, as shown in Fig. 6. Moreover, the effects of the branched nodes to these MTLs are replaced by controlled voltage sources.

It needs emphasis that these Norton circuits should affect each other inevitably due to the existence of mutual inductance and capacitance effects between these MTLs. Therefore, the equivalent circuit of the branched nodes is regarded as a multi-port network, as shown in Fig. 7, and the relationship between the port voltages and current sources of these Norton circuits is constructed by the admittance matrix, which is expressed as

$$\mathbf{GU}=\mathbf{I} \tag{14}$$

In Equation (14), $\mathbf{U}$ is the port voltage vector and expressed as $\mathbf{U}=[U_1,\ldots,U_i,\ldots,U_N]^T$, where N indicates the port number. $\mathbf{I}$ is the current source vector and expressed as $\mathbf{I}=[I_1,\ldots,I_i,\ldots,I_N]^T$, where $I_i=-\left(I_{SHi}+I'_{SHi}\right)$, and i stands for the i-th port of the network. $\mathbf{G}$ is the admittance matrix of the network, and the element values of $\mathbf{G}$ are computed by the equivalent admittance of these Norton

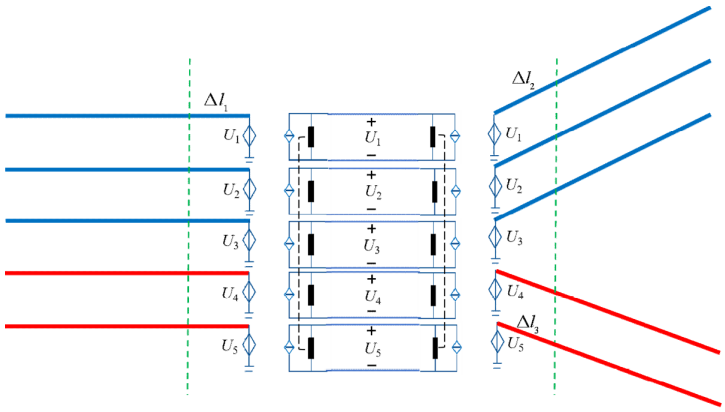

Figure 6. The whole equivalent circuit model of BLs.

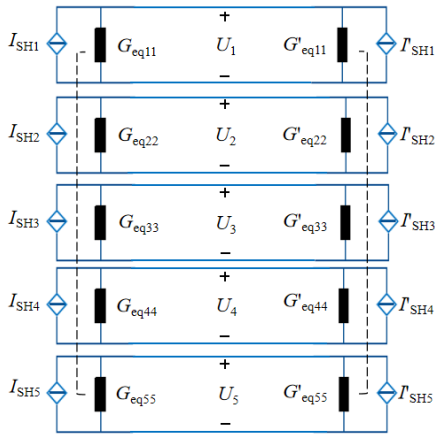

Figure 7. Admittance matrix construction of the port voltages of branched nodes.

circuits, which are written as $G_{ii} = \sum_{j=1}^{N} \left(G_{eqij} + G'_{eqij}\right)$ and $G_{ij} = -\left(G_{eqij} + G'_{eqij}\right)$, $i \neq j$, where G_{eqij} is obtained from the p.u.l capacitance matrices $\mathbf{C}_{\#1}$ of MTL#1 and expressed as

$$G_{eqij} = \Delta l_1 \cdot [\mathbf{C}_{\#1}]_{ij}/\Delta t, \quad i = 1, \ldots, 5, \quad j = 1, \ldots, 5 \tag{15}$$

Meanwhile, G'_{eqij} is computed by the p.u.l capacitance matrices of MTL#2 and MTL#3, and its corresponding matrix is expressed as

$$[\mathbf{G}'_{eq}] = \begin{bmatrix} \mathbf{G}_{\#2} & \mathbf{0} \\ \mathbf{0} & \mathbf{G}_{\#3} \end{bmatrix} \tag{16}$$

where

$$[\mathbf{G}_{\#2}]_{ij} = \Delta l_2 \cdot [\mathbf{C}_{\#2}]_{ij}/\Delta t, \quad i = 1, 2, 3, \quad j = 1, 2, 3 \tag{17}$$

$$[\mathbf{G}_{\#3}]_{ij} = \Delta l_3 \cdot [\mathbf{C}_{\#3}]_{ij}/\Delta t, \quad i = 1, 2, \quad j = 1, 2 \tag{18}$$

where $\mathbf{C}_{\#2}$ and $\mathbf{C}_{\#3}$ are the p.u.l capacitance matrices of MTL#2 and MTL#3, respectively. Δl_2 and Δl_3 are the grid sizes of MTL#2 and MTL#3 divided by the FDTD grid respectively, as shown in Fig. 6.

Then the voltages on the ports of the branched nodes can be solved by the inverse operation of Equation (14), which is expressed as

$$\mathbf{U} = \mathbf{G}^{-1}\mathbf{I} \tag{19}$$

3. NUMERICAL SIMULATION

In this section, the time domain hybrid method is adopted to simulate the coupling problems of ambient wave to the branched lines on the PEC ground and in the shielded enclosure, respectively. Then, the calculation results are compared with those of the traditional FDTD method to verify the correctness and efficiency of the proposed method.

The coupling model of five branched lines on the PEC ground excited by ambient wave is shown in Fig. 8, where the size of the ground plane is $L_c \times W_c = 1\,\text{m} \times 1\,\text{m}$, and the height, radius, and distance of the branched lines are 1 cm, 1 mm, and 1 cm, respectively. The angles between the directions of MTL#2 and MTL#3 with the horizontal direction are both 37°, and the terminal loads of the branched lines are $R_1 = R_2 = R_3 = R_4 = R_5 = 50\,\Omega$ and $R_6 = R_7 = R_8 = R_9 = R_{10} = 100\,\Omega$. The Gaussian pulse with magnitude 1000 V/m and pulse width 2 ns is perpendicular to the branched lines.

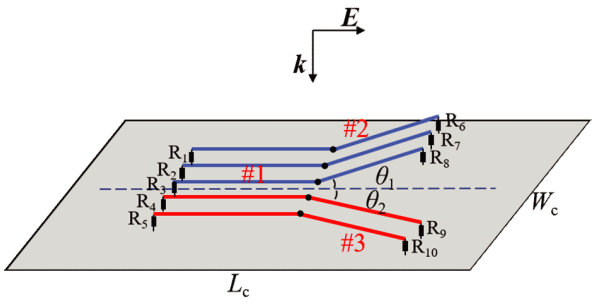

Figure 8. Coupling model of branched lines on the ground.

The hybrid method and FDTD method are utilized to compute the transient responses on the BLs and their terminal loads, and the comparisons of the voltages on the loads R_3 and R_9 are shown in Fig. 9, where good agreements of the results of the two methods can be found evidently. To further verify the accuracy of this proposed method, we assess the mean relative errors (MREs) of the voltage responses on all loads, as shown in Fig. 10. Here, MRE is defined as $\frac{1}{\mathrm{N}_0}\sum_{i=1}^{\mathrm{N}_0}\left(\left\|V^{real}(i) - V^{base}(i)\right\| / \left|V^{base}(i)\right|\right)$, where N_0 is the sampling point number of each load's voltage, and V^{real} and V^{base} are the voltage values obtained by the proposed method and FDTD method, respectively. $\|\cdot\|$ stands for the Euclidean norm.

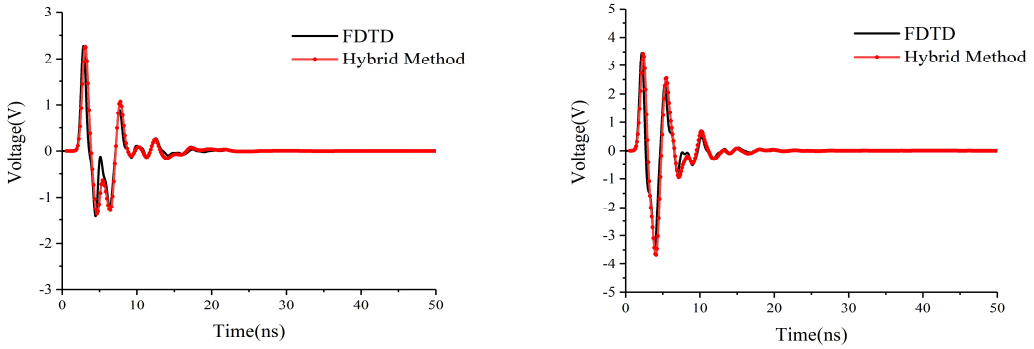

Figure 9. Terminal loads' voltages computed by the two methods for the first case: (a) voltage responses on R_3, (b) voltage responses on R_9.

We can see from Fig. 10 that the maximum MRE of the voltages of all loads is only 3.2%. It means that this hybrid method has the same precision as that of full wave algorithm.

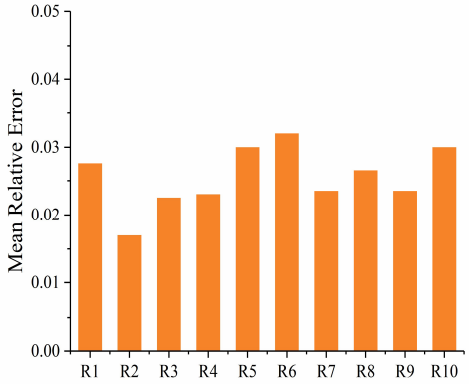

Figure 10. Mean relative errors of the voltages on all loads for the first case.

To further verify the efficiency of the proposed method, the grid number and computation time required by the two methods are compared in Table 1. Here, nonuniform grid technique is employed in the traditional FDTD method to improve the computation efficiency. It means using fine grid to mesh the branched line region and coarse grid to mesh other regions, where the fine grid size is 1 mm, and the maximum coarse grid size is 5 mm. Meanwhile, the grid size selected by the proposed method is 5 mm. We can see from Table 1 that the proposed method reduces certain computation time compared with the FDTD, because it can avoid directly meshing the fine structures of branched lines.

Table 1. Grid number and cost time required by the two methods for the first case.

Numerical Method	Grid Number	Cost Time (min)
FDTD	5.4×10^6	6
Hybrid Method	1.6×10^6	1.5

The coupling model of the branched lines in the shielded enclosure excited by ambient wave is shown in Fig. 11, where the dimension of the enclosure is $L_c \times W_c \times H_c = 100\,\text{cm} \times 100\,\text{cm} \times 50\,\text{cm}$. The upper surface of the enclosure contains three narrow slots with length 50 cm and width 5 cm. The structure parameters and terminal loads of the branched lines are the same as that of the first case. The incident wave is also a Gaussian pulse, and its wave parameters is the same as the first case, which is perpendicular to the upper surface of the enclosure.

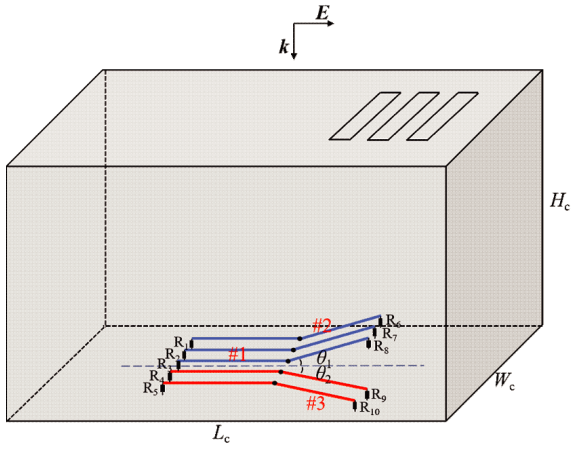

Figure 11. Coupling model of branched lines in shielded enclosure.

In the same way, the hybrid method and FDTD are used to compute the transient responses on the BLs and terminal loads. The comparisons of the voltages on the loads R_1 and R_9 obtained by the two methods are shown in Fig. 12. Meanwhile, all loads' voltage responses of the two methods are also estimated by the MRE analysis, as shown in Fig. 13. Obviously, the maximum MRE of the voltages of all loads is about 7.2%, which proves that this proposed method also has high precision even in complex electromagnetic environment.

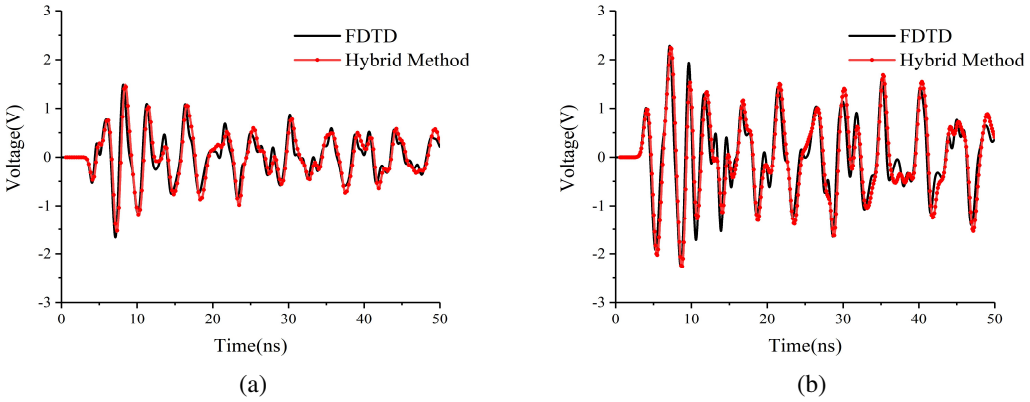

Figure 12. Terminal loads' voltages computed by two methods for the second case: (a) voltage responses on R_1, (b) voltage responses on R_9.

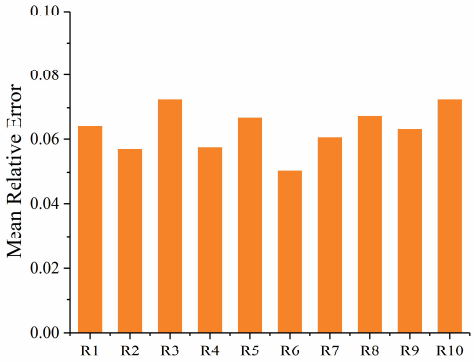

Figure 13. Mean relative errors of the voltages on all loads for the second case.

4. CONCLUSION

An efficient time domain field-circuit hybrid method is presented to solve the coupling problem of branched lines excited by space electromagnetic fields. Firstly, the branched lines are decomposed into independent MTL structures and branched nodes, and the whole equivalent circuit model of the branched lines is constructed via the Norton's theorem. Then, the coupling models of these MTLs are constructed by the TL equations and interpolation techniques, and the voltage and current responses on these MTLs are solved by FDTD to obtain the current sources and equivalent admittance of the Norton circuits. Finally, the admittance matrix representing the relationship of the port voltages of branched lines and current sources of Norton circuits is constructed, and then the port voltages are solved and fed back to the MTLs to realize the interference signal transmission of whole branched lines. Coupling simulations of the branched lines on the ground and in the shielded enclosure are employed to verify the correctness and efficiency of the proposed method by comparing with the traditional FDTD in terms of the simulation precision and computation time. In the future work, the skin effect and coupling effect of the branched lines will be fully considered in this method to further enhance its precision.

ACKNOWLEDGMENT

This work was supported by the Special Support for Chongqing Postdoctoral Research Project (Grant No. 2022CQBSHTB3018) and the Graduate Scientific Research Innovation Project of Chongqing(Grant No. CYS21297).

REFERENCES

1. Xie, L. and Y. Z. Lei, "Transient response of a multiconductor transmission line with nonlinear terminations excited by an electric dipole," *IEEE Transactions on Electromagnetic Compatibility*, Vol. 51, No. 3, 805–810, 2009.
2. Du, J. K., S. M. Hwang, and J. W. Ahn, "Analysis of coupling effects to PCBs inside waveguide using the modified BLT equation and full-wave analysis," *IEEE Transactions on Microwave Theory and Techniques*, Vol. 61, No. 10, 3514–3523, 2013.
3. Yan, L. P., X. D. Zhang, and X. Zhao, "A fast and efficient analytical modeling approach for external electromagnetic field coupling to transmission lines in a metallic enclosure," *IEEE Access*, Vol. 6, 50272–50277, 2018.
4. Nie, B. L., "Analysis of electromagnetic coupling to a shielded line based on extended BLT equation," *2019 Photonics & Electromagnetics Research Symposium — Fall (PIERS — Fall)*, 2934–2937, Xiamen, China, Dec. 17–20, 2019.
5. Paul, C. R., "A SPICE model for multiconductor transmission lines excited by an incident electromagnetic field," *IEEE Transactions on Electromagnetic Compatibility*, Vol. 36, No. 4, 342–354, 1994.
6. Erdin, I., A. Dounavis, and R. Achar, "A SPICE model for incident field coupling to lossy multiconductor transmission lines," *IEEE Transactions on Electromagnetic Compatibility*, Vol. 43, No. 4, 485–494, 2001.
7. Xie, H. Y., J. G. Wang, and R. Y. Fan, "SPICE models for prediction of disturbances induced by nonuniform fields on shielded cables," *IEEE Transactions on Electromagnetic Compatibility*, Vol. 53, No. 1, 185–192, 2011.
8. Chen, H. C., Y. P. Du, and M. Q. Yuan, "Lightning-induced voltages on a distribution line with surge arresters using a hybrid FDTD-SPICE method," *IEEE Transactions on Power Delivery*, Vol. 33, No. 5, 2354–2363, 2018.
9. Hu, X., Y. Qiu, L. Xu, and J. Tian, "A hybrid FDTD-SPICE method for predicting the coupling response of wireless communication system," *IEEE Transactions on Electromagnetic Compatibility*, Vol. 63, No. 5, 1530–1541, 2021.
10. Ye, Z. H., J. J. Zhou, and D. Gou, "Coupling analysis of ambient wave to the shielded cavity with penetrated wire using a time domain hybrid method," *Microwave and Optical Technology Letters*, Vol. 61, No. 11, 2551–2556, 2019.
11. Ye, Z. H., J. J. Zhou, and D. Gou, "Hybrid method for the EMI analysis of penetrated wire of electronic device excited by space electromagnetic fields," *Progress In Electromagnetics Research M*, Vol. 98, 213–221, 2020.
12. Meng, X. S., X. F. Bao, Y. T. Zheng, Q. Liu, R. Mittra, and H. J. Zhou, "Time-domain modeling of field-to-wire coupling in obliquely oriented multiwire cables with junctions using JEMS-FDTD," *IEEE Transactions on Electromagnetic Compatibility*, Vol. 62, No. 6, 2458–2467, 2020.
13. Wei, J. H., Y. J. Yan, S. T. Wang, T. Y. Jiang, and F. S. Gao, "FDTD-TL method for the prediction of the transient response of the shielded cable above the ground," *International Applied Computational Electromagnetics Society (ACES-China) Symposium*, 1–2, Chengdu, China, 2021.
14. Ye, Z. H., D. Gou, and J. J. Zhou, "Coupling analysis of oblique transmission lines excited by ambient wave with a time domain hybrid method," *12th International Workshop on the Electromagnetic Compatibility of Integrated Circuits (EMC Compo)*, 141–143, Hangzhou, China, 2019.

15. Ye, Z. H., X. L. Wu, and J. Zhang, "Time domain hybrid method for the coupling analysis of oblique transmission line network excited by ambient wave," *IEEE Transactions on Electromagnetic Compatibility*, Vol. 62, No. 6, 2450–2457, 2020.
16. Tesche, F. M., "On the analysis of a transmission line with nonlinear terminations using the time dependent BLT equation," *IEEE Transactions on Electromagnetic Compatibility*, Vol. 49, No. 2, 427–433, 2007.
17. Paul, C. R., *Analysis of Multiconductor Transmission Lines*, John Willy & Sons, New York, 1994.